Journal of Research in Health Sciences
ISSN: 2228-7809 | https://jrhsjournal.com

A Novel Assay for Identifying Therapeutics Targeting TTR and Amyloid-β Peptide Interactions

Dr. Lukas Fischer[1], Dr. Anna Becker[1], Dr. Jonas Wagner[2], Dr. Clara Hoffmann[2], Dr. Felix Braun[3], Dr. Marie Keller[3]*

[1]Charité University Hospital, Berlin, Germany

[2]University Hospital Frankfurt, Frankfurt, Germany

[3]University Hospital Munich, Munich, Germany

Abstract: By using animal models of Alzheimer Disease (AD) we have found that the protein transthyretin (TTR) modulates Abeta (A_i3) peptides deposition and processing. This physiological effect is further enhanced by treatment with iododiflunisal (IDIF) which is a small-molecule compound (SMC) with TTR tetramer stabilization properties. Further *in vitro* studies of the interactions of these three chemical entities by physicochemical methods (RMN and ITC) have revealed that TTR cooperatively binds to A_i3 leading to a stable protein-peptide complex that is chaperoned by IDIF. This knowledge has prompted us to design and optimize a rapid and simple high-throughput assay that relies on the ability of test compounds to form ternary soluble complexes TTR/A_i3/SMC that prevent A_i3 aggregation. The method uses the shorter A_i3(12-28) sequence which is cheaper and simpler to use while retaining the aggregation properties of their parents A_i3(1-40) and A_i3(1-42). The test is carried out in 96 plate wells that are UV monitored for turbidity during 6 h. Given its reproducibility, we propose that this test can be a powerful tool for efficient screening of SMCs that act as chaperones of the TTR/A_i3 interaction that may led to potential AD therapies.

INTRODUCTION

Transthyretin (TTR) is a homotetrameric protein found in the plasma and cerebrospinal fluid (CSF) that transports thyroid hormones and retinol [1]. It is most stable as a tetramer, but many point mutations are involved in pathological conditions caused by toxic TTR amyloid deposits in vital organs [2,3]. It is relevant to note that TTR is the main A-beta (A¡3) binding protein in CSF [4,5]. This binding is believed to naturally prevent A¡3 aggregation and toxicity in this fluid. This first physiological evidence suggesting a putative neuroprotective effect of TTR has been later confirmed by a number of biochemical and animal studies as well as comparative measures of TTR levels in healthy and AD patients [6-8]. The molecular mechanisms of TTR neuroprotection have not been fully elucidated. Recent data suggests that TTR interferes with Aφ3 by redirecting oligomeric nuclei into non-amyloid aggregates [9]. Also, TTR seems to inhibit both primary and secondary nucleations of A¡3 peptides aggregation reducing the toxicity of their oligomers [10].

In early *in vitro* studies we have gathered a first insight of the binding of TTR and A¡3 and on this binding enhancing role of a small set of TTR tetramer-stabilizing compounds [11]. One of the compounds is an iodinated analogue of the nonsteroidal anti-inflammatory drug (NSAID) diflunisal namely, iododiflunisal (IDIF) [12-14]. Later, we have shown that *in vivo* administration of IDIF to AD transgenic mice, resulted in binding and stabilization of the TTR tetramer, decreasing brain A¡3 levels and deposition and improving the cognitive functions that are impaired in this AD-like neuropathology [15]. By very recent radiochemical studies, we have proved that preformed TTR-IDIF labelled complexes better penetrate the blood brain barrier (BBB) than free TTR and IDIF [16].

To elucidate at the molecular level the mechanisms involved in these TTR/A¡3/IDIF interactions by biophysical methods we have used Saturation-Transfer Difference nuclear magnetic resonance (STD-NMR) techniques that have allowed us to identify the 17-mer peptide sequence A¡3(12-28) as the main structural recognition motif [17]. Interestingly, this short A¡3 amyloid peptide (VHH QKLVF FAEDV GSNK) has been extensively studied and is reported to exhibit essentially identical neurotoxic behavior and fibril formation features as the A¡3(1-42) and (1-40) peptides and thus has been used as a short model of the full A¡3 peptides [18-20]. Structural studies of this A¡3(12-28) amyloid sequence have shown to contain a domain known as the "hydrophobic core" (residues 17-21) and a ¡3-turn (residues 22-28) [21-23]. These peptide stretches look essential for the formation of large aggregates and fibrils in the Aφ3(1-40) and Aφ3(1-42) longer peptides [24-25]. Thus, mutations in the hydrophobic core such as Phe19/Pro19 have a large influence on the aggregation properties and even prevent fibrillization [26]. Also, the aggregation characteristics of A¡3(12-28) have a strong pH dependence [27-28]. Interestingly, this same A¡3(12-28) sequence has also been identified among the key determinants for the recognition of full A¡3s by other amyloid binding proteins, such as ApoE [29-30] and HSA [31].

Furthermore, in our biophysical studies of these ternary interactions we have also used isothermal titration calorimetry (ITC) techniques that have provided conclusive proof of stable complex formation in solution between these TTR, A¡3 and IDIF molecular species. Thus, both A¡3(1-42) and A¡3(12-28) do not bind with IDIF but form binary complexes with TTR. In turn, binary

TTR/IDIF complexes bind more effectively than TTR alone with A¡3 species to form ternary complexes. This more effective binding provided by IDIF allow us to talk about a chaperoning effect of IDIF upon TTR/A¡3 binding [32].

With this information at hand, we envisioned a simple ternary reaction system composed by TTR, A¡3(12-28) and a SMC acting as chaperone that could be easily monitored for aggregates formation in a high throughput screening (HTS) format that could allow to screen for other chaperones. In such a system the chaperone could prevent aggregate formation through soluble ternary complex formation and the extent of precipitate formation could be an indirect measure of the chaperone potency. For setting such a system we have revisited our former turbidimetric method for screening of potential TTR fibrillogenesis inhibitors. Our method used a mutant TTR and was optimized as to carry kinetic monitoring of TTR aggregation by simply measuring the turbidity of 96 plate wells by UV. Turbidimetry kinetics were used to assess the potency of fibrillogenesis inhibition compounds [33].

In this case, to design a simple and rapid assay, turbidity appeared again a good choice for reaction monitoring. Thus, given that native TTR is a thermostable protein that does not show amyloid properties in solution at neutral pH, we aimed at measuring the ability of a particular test compound to prevent aggregation of the A¡3(12-28) peptide in solutions also containing TTR. As here described, we have first optimized the operating conditions for A¡3(12-28) aggregation by using common methods of rational Design of Experiments (DoE) [34-35]. Secondly, convenient A¡3(12-28)/TTR/SMC molar ratios as to discriminate the effect of different SMCs acting as TTR ligands were sought. The final assay setup comprises incubation of different test compounds with solutions containing both TTR and A¡3(12-28) as to allow the formation of the ternary complexes in a 96-well format and the turbidimetry of the wells monitored for 6 hours by measuring the absorbance at 340 nm. Turbidimetry is used as a measure of the chaperoning potency of the SMCs.

It is known that A¡3 peptides interact and form complexes with proteins other than TTR such as: Gelsolin [36], ApoJ (clusterin) [37-38], ApoE [39] and human serum albumin (HSA) [40-41]. These complexes also seem to interfere with A¡3 aggregation and therefore may constitute a new therapeutic target for AD. Owing the urgent need to feed the exhausted pipelines of drug candidates for AD (see Supplementary Information, 1) we propose that the methodology here described, besides its potential for the discovery of TTR/A¡3 interaction modifying SMCs, may be inspiring to settle new screening methods for potential AD therapeutic interventions based on other A¡3 interacting proteins.

RESULTS AND DISCUSSION

Materials. Relative high quantities of the synthetic Abeta(12-28) peptide and recombinant TTR were a requisite por this study. Thus, the A¡3(12-28) amyloid peptide was in house synthesized at mM scale by microwave solid-phase peptide synthesis (SPPS) protocols. Preparation of recombinant TTR was achieved by expression in *Escherichia coli* following our previously described methods, with slight modifications to increase protein production [33]. Yield of pure

protein was 150 mg/L of culture and a batch of 500 mg was produced (see Supplementary Information).

Preliminary Experiments. In a preliminary set of experiments the aggregation of separated A¡3(12-28) and TTR solutions were compared with (2:1) molar mixtures of A¡3(12-28) and TTR which were kept at 37 ºC under stirring in a neutral buffer and monitored at 340 nm for turbidity during 6 h. It was observed that the peptide readily aggregates reaching a maximum in less than 3h, TTR solutions remained clean and (2:1) peptide/protein mixtures produced a faint precipitate.

Also, additional mixtures of A¡3(12-28) and TTR where challenged with IDIF. Thus, IDIF was incubated with TTR solutions at (1:2) molar ratios and then added to A¡3 peptide solutions at (2:1) peptide/protein ratios. No aggregates could be detected after 6 h (see SI Figure S3) and up to 18 h (see SI Fig. S6). In addition, equimolar mixtures of A¡3/IDIF and TTR/IDIF were prepared and monitored for turbidity to confirm that IDIF is not able to prevent A¡3 aggregation nor to induce TTR aggregation (see SI Figure S6).

Optimization of AP(12-28) aggregation. Having in mind that maximal sensitivity of aggregate detection by turbidimetry and minimal cost of reagents were very important factors, the HTS assay here described has been settled and optimized in two stages. In a first stage, the aggregation conditions of the A¡3(12-28) peptide were selected and optimized. Thus, the following parameters: incubation temperature, nature and ionic strength of buffer solution, concentration of A¡3(12-28) and selection of UV wavelength monitoring were either individually or collectively optimized by rational DoE methods. In a second stage, the optimal peptide aggregation conditions where used as to find the most suitable A¡3(12-28)/TTR/SMC ratios for optimal assay output.

To identify the optimum wavelength that better differentiates between soluble and aggregated peptide we have performed spectral scannings (260-440 nm) on 200 µM solutions of A¡3(12-28). One run was performed immediately after preparation of the solution and the second after standing at 37 ºC for 6h (see SI Figure S4). The maximum absorption difference between the initial clean solution and the turbid final solution was observed at 340 nm. This wavelength is in the 340-360 nm range, which has been used to characterize other amyloid aggregation processes and therefore was adopted as optimal for our study [42-44].

For the optimization of the rest of the factors, this is, incubation temperature, ionic strength of buffer and concentration of peptide a factorial DoE was used. Reaction temperature and ionic strength, were analyzed at two levels while concentration of reagents at three resulting in a ($3^1 2^2$) factorial design (see S.I. Tables S1, S2 and S3). Accordingly, a total of 12 experiments that were repeated 3 more times with a sum of 48 runs. In addition, the block effect, this is, the influence of different batches of the peptide was also taken into account.

For each experiment, the mean value of the absorbance at 340 nm after 6 hours of reaction was taken as the variable response. The design and analysis of results were performed using the

JMP software package (SAS Institute) [45] while statistical significance was assessed by ANOVA (see S.I. Table S4). It was found that all the main factors (concentration, ionic strength and temperature) and the interactions between concentration and the other two factors were statistically significant but not the temperature versus ionic strength interaction. As expected, the block factor was not statistically significant (see S.I. Table S5).

As seen from prediction profiles and desirability plots (see S.I. Figure S5) the most influential factor on absorbance was the peptide concentration. This can be seen from the examples of reaction profiles at different conditions provided in Figure 1. To reduce economic costs a concentration of 100 μM of the peptide was selected for subsequent experiments. The other two factors were fixed at their low level (temperature at 37 ºC and ionic strength at 0 μM).

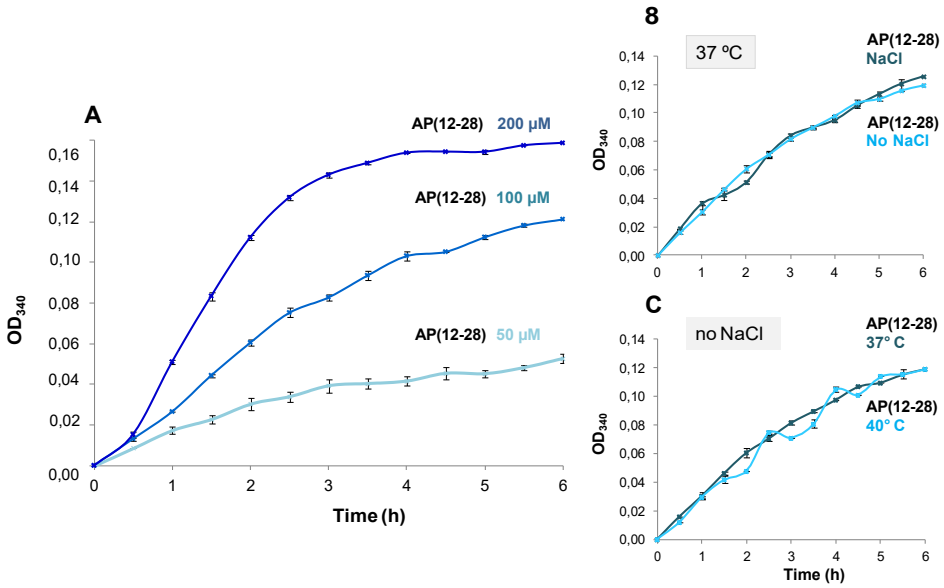

Figure 1. Aggregation kinetics of A¡3(12-28) peptide at 37 ºC monitored by UV (340 nm) over 6h. A) At 50, 100 and 200 μM concentrations. B) In absence or presence of salts ([NaCl] = 100 mM). C) At different temperatures and absence of salts. Samples were assayed in duplicate and are representative of three (n = 6) (A) or two different experiments (n=4) (B and C). Studies performed at pH 7.4 in 25 mM HEPES buffer, 10 mM glycine and 5% DMSO (final concentration) at 37 ºC.

Assay optimization. After setting the optimal A¡3(12-28) aggregation conditions, in a second stage of the assay development the most convenient peptide/protein ratio that may allow discrimination between different SMCs that act as TTR ligands was sought. Thus, in view of the preliminary experiments shown in Figure S3, that used a (2:1) stoichiometric peptide/protein ratio, a discrete range of A¡3(12-28) to TTR ratios going from an excess of peptide (4:1) to an excess of protein (1:2) were investigated (Figure 2A). Similar range of peptide/protein ratios were also studied in the presence of the TTR ligand IDIF (Figure 2B, 2C and 2D). From Figure 2B, it appears that the (2:1) peptide/protein ratio seems rather convenient for the quantification of the chaperoning effect of IDIF. In turn, this ratio also allows for a moderate consumption of protein.

In addition, we have firm evidence from isothermal titration calorimetry (ITC) experiments that in these conditions ternary A$_i$3(12-28)/TTR/IDIF complexes are formed [32].

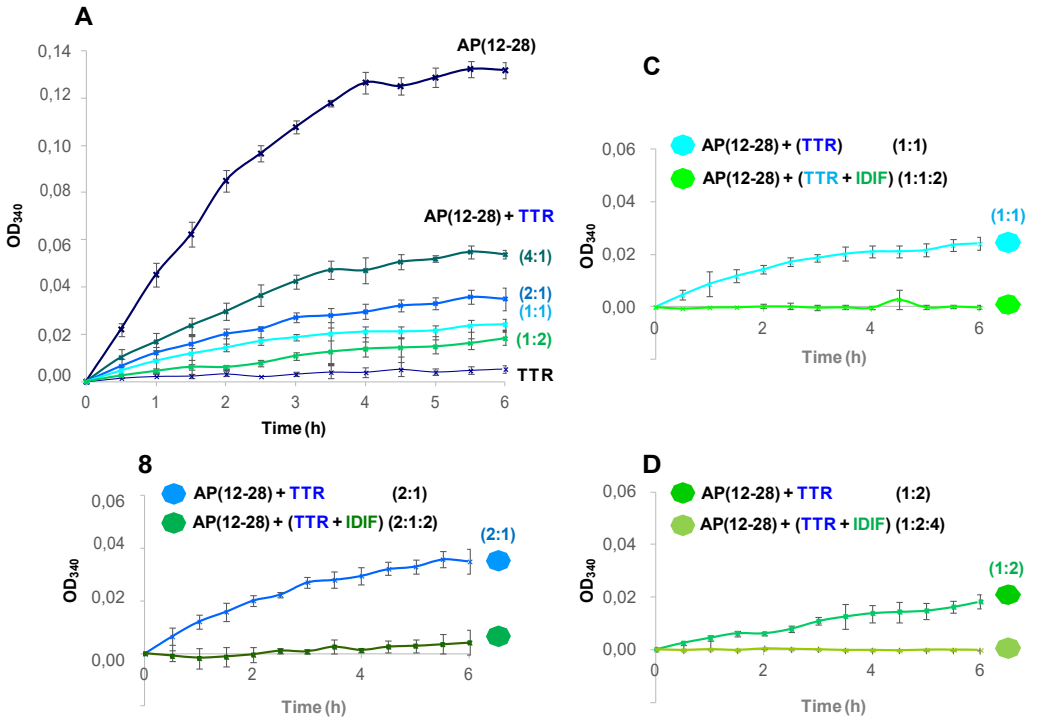

Figure 2. A) Kinetic profiles of the aggregation of A$_i$3(12-28), TTR and Aφ3(12-28)/ TTR mixtures at (4:1), (2:1), (1:1) and (1:2) molar ratios; B) A$_i$3(12-28) aggregation course at (2:1) A$_i$3(12-28)/ TTR molar ratio with or without IDIF (2 molar); C) A$_i$3(12-28) aggregation course at (1:1) A$_i$3(12-28)/ TTR molar ratio with or without IDIF (2 molar); D) A$_i$3(12-28) aggregation course at (1:2) A$_i$3(12-28)/ TTR molar ratio with or without IDIF (4 molar), measured by turbidity at 37 ºC over 6 h. Samples were assayed in duplicate and are representative of two different experiments (n=4). All of them performed at pH 7.4 in 25 mM HEPES buffer, 10 mM glycine and 5% DMSO (final concentration) at 37 ºC.

HTS Assay Development. This information was next translated into a working HTS assay using 96-well microplates (See SI Scheme S2). In doing so, in each plate different positive and negative controls were always included. In particular, the A$_i$3(1-11) sequence which does not show aggregation was taken as a negative control. It was always checked that TTR ligands alone do not modify the A$_i$3(12-28) aggregation process.

The concentration of the test compounds in the assay was selected based on previous knowledge of their binding stoichiometry to the tetrameric form of TTR which is either (1:1) or (1:2) protein/ligand. A small quantity of DMSO (5% final concentration) was always added to buffered stock solutions of ligands to improve their solubility.

The protocol operation started with the incubation of the SMC (100 µM) with the protein (50 µM) for one hour at 37 ºC followed by addition of A$_i$3(12-28) (100 µM) and then the plate was incubated for 6 h at 37 ºC.

Profiles of control experiments as well as results from a typical experiment using IDIF as a SMC ligand using optimal assay conditions are presented in Figure 3.

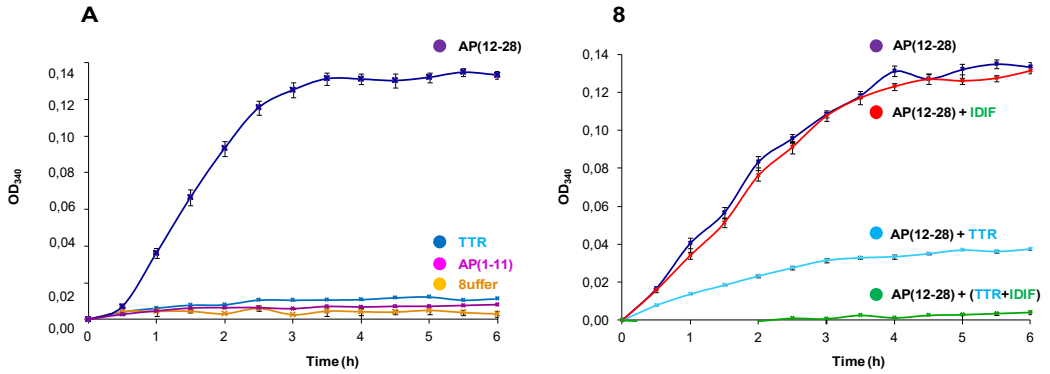

Figure 3. Aggregation kinetics of the A¡3(12-28) peptide measured using the HTS operating format in a 96-well plates: A) Control experiments: dark blue, A¡3(12-28) (100 µM); light blue, TTR (50 µM); pink A¡3(1-11) and yellow, buffer. B) dark blue, A¡3(12-28); red, A¡3(12-28) with IDIF; light blue, A¡3(12-28) with TTR (binary complex); green, A¡3(12-28) plus TTR/IDIF mixture (ternary complex). Samples were assayed in duplicate and results are representative of three different experiments (n=6). Studies were performed at pH 7.4 in 25 mM HEPES buffer, 10 mM glycine and 5% DMSO (final concentration) at 37 ºC.

Quantitative results are calculated from the UV absorbance of each well after 6 hours. The potency of a test compound is expressed as the percentage of reduction of the UV absorbance observed for a the compound when compared to an A¡3(12-28) aggregation control experiment. Thus, the potency of IDIF is 96% (Table 2).

Table 2. Quantification of SMCs potency.

	OD_{340}	p-value[1]	Reduction of aggregation (%) (RA ± SD %)
A¡3(12-28)	0.131 ± 0.009		0
A¡3(12-28) + TTR	0.028 ± 0.004	0.000*	79 ± 2.5
A¡3(12-28) + [TTR + IDIF]	0.006 ± 0.005	0.000*	96 ± 1.4

[1] Statistically significant factors and interactions are those whose p-value < 0.05; p-value obtained using the non-parametric Wilcoxon rank-sum test [46].

Analysis of the Z'-factor for the assay [47] gave values of 0.9 for IDIF and of 0.87 for TTR meaning that the assay is well-suited for HTS.

Alternative assay monitoring. Following the assumption that A¡3(12-28) aggregation yields amyloid structures, monitoring of the assay was also investigated using Thioflavin-T (ThT) fluorescence. Given that ThT tightly binds to amyloid structures, this method is widely accepted and used for the characterization of amyloid aggregates [48]. As seen in Figure 4 the kinetic patterns of A¡3(12-28) aggregation in the different conditions of the assay are consistent with the formation of amyloid structures which are greatly reduced by TTR/IDIF complexes. These patterns are un good accordance with the ones obtained by UV monitoring.

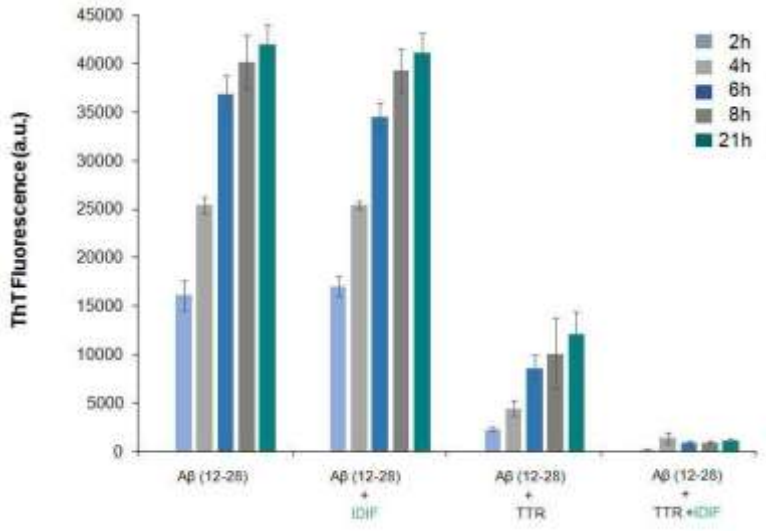

Figure 4. ThT fluorescence monitoring of the aggregation of A¡3(12-28). Kinetic course of A¡3(12-28) only; A¡3(12-28) in the presence of IDIF; A¡3(12-28) in complex with TTR and in complex with TTR stabilized with IDIF. ThT fluorescence was measured at 37 ºC at different time intervals. Studies were performed at pH 7.4 in 25 mM HEPES buffer, 10 mM glycine and 5% DMSO (final concentration) at 37 ºC.

To further investigate the nature of the A¡3(12-28) aggregates formed in the different assay conditions a morphological analysis by transmission electron microscopy (TEM) was performed. The ultrastructural examination revealed that after 48 h of incubation at 37 ºC, A¡3(12-28) formed highly ordered and structured fibrils. However, in the presence of TTR/IDIF complexes only round and small particles were observed (See S.I. Figure S9).

It is well established that A¡3 peptides and its oligomeric forms are toxic to neural cells leading to apoptosis and cellular death. It is also settled that TTR protects against this neurotoxicity [49, 9, 10]. Caspase-3 activation is one of the methods to measure this toxicity. Using caspase-3 activation tests on the samples of our screening test we have observed that TTR can reduce up to 45% the levels of caspase-3 activation while the TTR/IDIF complex effect is about 60**%** (See S.I. Figure S10).

Assay validation. To examine the proficiency of the assay to discriminate among structurally different SMC, a small set of TTR ligands was selected and tested (Figure 5). Two of them, tafamidis and diflunisal are licensed drugs. The *N*-aryl anthranilic acids, *N*-(3,5-dichlorophenyl)anthranilic acid (DCPA) and the *N*-(3,5-difluorophenyl)anthranilic acid (DFPA) were chosen because of their good TTR binding properties [11]. As seen in Figure 5D, 5E and 5F, among the four products, DCPA and DFPA show extensive chaperone properties similar to IDIF. Given that these three compounds are good TTR tetramer stabilizers, this condition seems a reasonable preliminary indication for the selection of potential chaperones entering the assay.

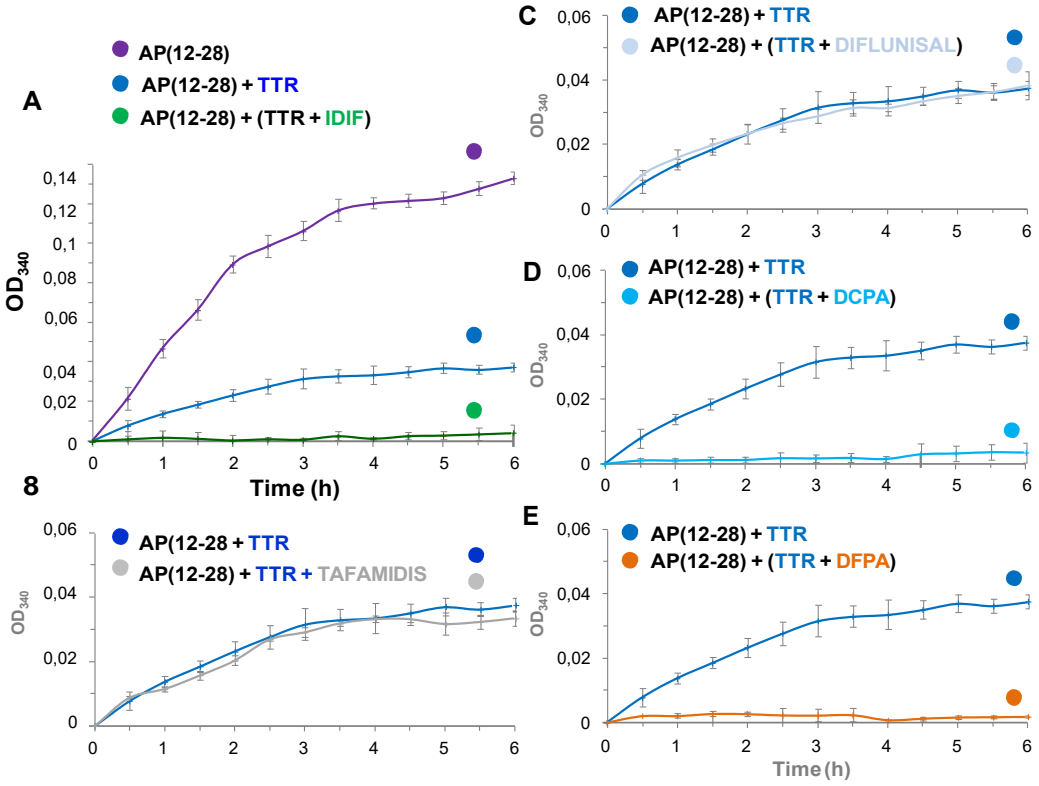

F	OD_{340}	Reduction of aggregates (RA ± SD%)
A_i3(12-28)	0.131 ± 0.009	0
A_i3(12-28) + TTR	0.028 ± 0.004	79 ± 2,5
A_i3(12-28) + [TTR+DIF]	0.032 ± 0.004	80 ± 3,0
A_i3(12-28) + [TTR+IDIF]	0.006 ± 0.005	96 ± 1,4
A_i3(12-28) + [TTR+TAFAMIDIS]	0,031 ± 0.001	81 ± 0,6
A_i3(12-28) + [TTR+DCPA]	0.004 ± 0.002	97 ± 1,5
A_i3(12-28) + [TTR+DFPA]	0.002 ± 0.002	98 ± 1,6

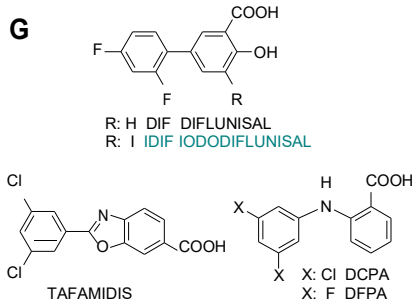

Figure 5. Aggregation kinetics of A_i3(12-28) mediated by the four selected SMC as measured by the turbidity assay at 37 ºC over 6 h. Chaperoning effect of: A) IDIF, B) tafamidis, C) diflunisal, D) DCPA, and E) DFPA. Samples were assayed in duplicate and are representative of two different experiments (n=4). Studies were performed at pH 7.4 in 25 mM HEPES buffer, 10 mM glycine and 5% DMSO (final concentration) at 37 ºC. F) Parameters for aggregation from the turbidimetric assay. G) Chemical structures of the SMCs assayed.

These aggregation kinetics of A_i3(12-28) in the presence of the four selected SMC have also been monitored by ThT fluorescence giving coherent results with the turbidity measurements (See S.I. Fig. S8). Furthermore, ITC techniques has been used to corroborate the formation of the corresponding A_i3(12-28)/TTR/SMC ternary complexes with the four selected compounds (see SI Fig. S14 and S15).

CONCLUSIONS

The interaction of TTR with A¡3 peptides is well established. We and others have consistently proven that this interaction is neuroprotective by preventing A¡3 aggregation and consequent cytotoxicity. We have provided firm evidence that this interaction can be further enhanced by IDIF, a SMC. For the search of other SMCs that may also be good chaperones of the TTR/A¡3 peptides interaction be have designed and implemented an HTS. The assay here described makes use of the more simple, easily handling and less costly A¡3(12-28) peptide than the full-length A¡3 peptides. The assay monitors A¡3(12-28) aggregation in the presence of both TTR and a SMC which is a TTR ligand that acts as chaperone of the A¡3(12-28)/TTR interaction. The aggregation kinetics can be monitored with parallel results by either the turbidity of the solutions as detected by UV or ThT fluorescence of the amyloid structures formed.

The assay has been optimized for: 1) UV wavelength monitoring (340 nm), 2) A¡3(12-28) aggregation factors (concentration of peptide, buffer solution, incubation temperature) by using a factorial DoE of ($3^1 2^2$) and 3) TTR/ A¡3(12-28) ratio as to minimize protein expenditure.

The assay has been adapted to a 96-well plate format and tested using a set of 4 compounds that have different TTR binding properties. It was observed that TTR ligand ability correlates with chaperone efficiency of the A¡3(12-28)/TTR interaction. Chaperones always form ternary complexes A¡3(12-28)/TTR/SMC as seen by ITC.

We propose that this assay may be a simple and effective tool for screening chaperones of the A¡3 peptides/TTR interactions that may constitute potential AD therapeutic agents. We also hope that the methodology here described may be inspiring to settle screening methods for chaperones acting on other proteins interacting with A¡3 peptides.

MATERIALS AND METHODS

Chemical compounds.

Dimethyl sulfoxide (DMSO); *N*-(2-hydroxyethyl) piperazine-N'-(2-ethanesulfonic acid) (HEPES); glycine; Tris(hydroxymethyl)-aminomethane (Tris); TFA, Trifluoroacetic acid and dimethyl sulfoxide (DMSO) were acquired from Sigma Aldrich. The small-molecule compound iododiflunisal (IDIF), an iodinated analogue of the NSAID diflunisal was synthesized in our lab IQAC-CSIC following our reported procedures [13]. The NSAIDs diflunisal (DIF) and *N*-(3,5-dichlorophenyl)anthranilic acid (DCPA) were from Sigma-Aldrich (diflunisal, D3281; DCPA, D8942; purity 298%. The small-molecule *N*-(3,5-difluorophenyl)anthranilic acid (DFPA) was prepared in our lab as previously described [11]. Purity of all final compounds was proved to be 295% by means of HPLC, HR-MS, and NMR techniques. Stocks of compounds assayed as small molecule ligands were dissolved in DMSO (ACS spectrophotometric grade, Sigma 154938) to a final 10 mM concentration. Working solutions of ligands were prepared by taking an aliquot of 50 μl of the DMSO (5%) stock solution and diluting it with 950 μl of buffer A (25 mM HEPES buffer, 10 mM glycine, pH 7.4 was prepared in the absence of salt), ratio (1:20), equivalent to a 500 μM concentration of ligand.

Amyloid peptides.

The amyloid peptide sequences A¡3(1-11) and A¡3(12-28) were purchased from Bachem AG (Switzerland) as trifluoroacetate salts (ref. H-2956 and H-7910, respectively. Purity by HPLC > 95%). The A¡3(12-28) peptide was also synthesized by Microwave Solid-Phase Peptide Synthesis (MW-SPPS) using Fmoc chemistry using the corresponding Fmoc protected amino acids. Cleavage from resin was performed using TFA/$H_2$0/TIS (95:2,5:2,5) (V:V:V) and the peptide was precipitated with *tert*-butyl methyl ether. The peptide was purified by RP-HPLC using a VersaFlash® system and characterized by analytical RP-HPLC and UPLC-ToF MS and compared to the commercial sample acquired from Bachem (H-7910).

Recombinant wild-type human TTR (wt rhTTR) production and purification.

Human wild type rhTTR gene was cloned into a pET expression system and transformed into *E. coli* BL21(DE3) Star. The phTTRwt-I/pET-38b(+) plasmid was provided by Prof. Antoni Planas (IQS, URL). The production of recombinant protein was performed at Erlenmeyer scale, protein production and purification were done as described previously following an optimized version of our protocol (see SI Scheme S1) [33]. wt rhTTR was produced using a pET expression System. The expressed protein only contains an additional methionine on the *N*-terminus if compared to the mature natural human protein sequence. wt rhTTR protein was expressed in *E. coli* BL21-(DE3) cells harboring the corresponding plasmid. Expression cultures in 2xYT rich medium containing 100 µg/mL kanamycin were grown at 37 ºC to an optical density (at 600 nm) of 4 (0D600=4), then induced by addition of IPTG (1 mM final concentration), grown at 37 ºC for 20 h, and harvested by centrifugation at 4 ºC, 10000 rpm for 10 min and resuspended in cell lysis buffer (0,5 M Tris-HCl, pH 7.6). Cell disruption and lysis were performed by French press followed by a sonication step at 4 ºC. Cell debris were discarded after centrifugation at 4 ºC, 11000 rpm for 30 min. Intracellular proteins were fractionated by ammonium sulfate precipitation in three steps. Each precipitation was followed by centrifugation at 12 ºC, 12500 rpm for 30 min. The pellets were analyzed by SDS-PAGE (14% acrylamide). The TTR-containing fractions were resuspended in 20 mM Tris-HCl, 0.1 M NaCl, pH 7.6 (buffer A) and dialyzed against the same buffer. It was purified by Ion exchange chromatography using a Q-Sepharose High Performance (Amersham Biosciences) anion exchange column and eluting with a NaCl linear gradient using 0.1 M NaCl in 20 mM Tris-HCl pH 7.6 buffer A to 0.5 M NaCl 20 mM Tris-HCl pH 7.6 (buffer B). All TTR-enriched fractions were dialyzed against deionized water in three steps and were lyophilized. The protein was further purified by gel filtration chromatography using a Superdex 75 prep grade resin (GE Healthcare Bio-Sciences AB) and eluting with 20 mM Tris pH 7.6, 0.1 M NaCl. Purest fractions were combined and dialyzed against deionized water and lyophilized. The purity of protein preparations were >95% as judged by SDS-PAGE. Average production yields were 150-200 mg of purified protein per liter of culture. Protein concentration was determined spectrophotometrically at 280 nm using calculated extinction coefficient value of 17780 $M^{-1}{\cdot}cm^{-1}$ for wtTTR. The protein was stored a -20 ºC.

Turbidity assay.

In this assay the following stock solutions were used: Buffer A: 25 mM HEPES buffer, 10 mM glycine, pH 7.4 was prepared in the absence of salt. Protein (TTR) stock: 9,5 mg/mL (170 µM) in 25 mM HEPES buffer, 10 mM glycine, pH 7.4 and 5% DMSO (final concentration) was prepared in the absence of salt (buffer A). For the *Aφ3 peptide stock*: 0,4 mg/mL (200 µM) in 25 mM HEPES buffer, 10 mM glycine, pH 7.4 and 5% DMSO (final concentration). For the small-molecule compound IDIF, a first solution of 3,76 mg/mL (10 mM) in DMSO was prepared. The final stock of the small-molecule IDIF was prepared by mixing 50 µL of the previous DMSO solution with 950 µL of buffer A (the final concentration of 5% DMSO).

First, the small-molecule compound and TTR complex was formed. To this end, 60 µL of TTR stock was dispensed into the wells of a 96-well microplate. 40 µL of small-molecule stock was added to give final concentrations of 100 µM. The plate was introduced in the microplate

reader (SpectraMax M5 Multi-Mode Microplate Readers, Molecular Devices Corporation, California, USA) and incubated for 1h at 37 ºC with orbital shaking 15 s every 30 min. Then, 100 µL of A¡3 solution was added to the well to give a final concentration of 100 µM.

Other wells of the 96-well microplate are filled with: a) Buffer alone: 200 µL of buffer A solution was added to the well; b) Negative control of Aφ3 aggregation: 200 µL of A¡3(1-11) stock solution in buffer A was dispensed into the wells; c) Testing TTR aggregation: 60 µL of TTR stock were dispensed into the wells of a 96-well microplate and 140 µL of buffer A were added; d) For the A¡3(12-28) aggregation: 100 µL of A¡3(12-28) stock solution is dispensed into the wells and 100 µL of buffer A were added.

The plate was incubated at 37 ºC in a thermostated microplate reader with orbital shaking 15 s every minute for 30 min. The absorbance at 340 nm was monitored for 6 h at 30 min intervals. Data were collected and analyzed using Microsoft Excel software. All assays were done in duplicate.

$$\left.\left.\frac{\qquad\qquad}{Abs_{A\square} + Abs_c}\right)\right] * 100 \qquad (1)$$

The parameter monitored in this assay was used to calculate the percent reduction of formation of aggregates (RA %) according to equation 1, where $Abs_{A¡3}$ and Abs_c are the final absorbance of the samples, in the absence or in the presence of the small-molecule compound/TTR complex; respectively.

Statistical analysis

The quality of an assay for HTS can be evaluated based on the Z'-factor [47] which reflects the separation in mean values for the high and low controls while taking into consideration the variability within each group. A Z' factor below zero indicates poor quality assay with no separation between the high and low controls. A Z' factor value between 0.5 and 1 indicate an excellent quality assay with large separation between the high and low controls. Preferably, optimized assays have a Z' value above 0.5. The statistical Z'-factor can be calculated using equation 2:

$$Z' = 1 - \frac{3SD\,of\,sample + 3SD\,of\,control}{!mean\,of\,sample - mean\,of\,control!} \qquad (2)$$

where sample is the highest RA% for A¡3(12-28) in presence of the binary complex (TTR+IDIF) or TTR alone, and the control is the A¡3(12-28) aggregation. "Mean" is the mean value of the aggregation after 6 h, and SD is the standard deviation.

Design of experiments (DoE)

Factorial designs are one of the most important DoE because they produce efficient experiments that allow observation of responses to one factor at different levels of other factors in the same experiment [59-60]. A factorial design of experiments was employed using the statistical software JMP 12.1.0 (SAS Institute) [45]. The variable to be maximized was the absorbance. Three factors were investigated: the concentration (µM), the temperature (ºC) and the ionic strength (mM of NaCl). Preliminary investigations were carried out to select initial analysis conditions, taking into account that temperature and ionic strength may have a nonlinear effect on the fibril formation, we have considered these two factors in a two-level design, the temperature at 37 ºC and 40 ºC and the ionic strength ([NaCl]) at 0 and 100 mM. The concentration was considered at three levels 50, 100 and 200 µM, to identify the sensitivity of our method. The UV absorption maxima for A¡3-peptide fibril formation is achieved at 340, 360 and 405 nm. Specific experimental conditions tested, and the flow layout of a Design of Experiments can be found in the Supporting Information (SI Scheme S3).

Thioflavin-T fluorescence assays

The robustness of our turbidimetry-based method was further validated on the basis of comparative by Thioflavin-T (ThT) fluorescence assays on the same system. The ThT fluorescence was monitored at 37 ºC using Gemini XPS plate reader (Molecular Devices) at an excitation wavelength of 440 nm and an emission wavelength of 490 nm. Thioflavin-T (ThT) was dissolved in 25 mM HEPES buffer, 10 mM glycine, pH 7.4 and 5 % DMSO to a final concentration of 25 μM. Aggregation of A¡3(12-28) 50 μM was performed in the presence of 25 μM ThT. All solutions were dissolved in the same buffer. TTR was added to a final concentration of 25 μM. IDIF was added to a final concentration of 50 μM. For the ternary complex, TTR was incubated first with IDIF for 1h, then A¡3(12-28) was added. The final volume was 200 μL for all samples. Fluorescence intensity at 490 nm of each sample was monitored after each 2h for 8h, and then at 21h. Measurements were performed as independent triplicates. Recorded values were averaged and background measurements (buffer containing 25 μM ThT) were subtracted. Measurements were performed as independent triplicates. Recorded values were averaged and background measurements (buffer containing 25 μM ThT) were subtracted.

Transmission Electron Microscopy (TEM)

A¡3(12-28) peptide (100 μM), alone or with TTR (20 μM) (alone or pre-incubated with IDIF for 1 hour at 37 ºC) was incubated at 37 ºC for 48 h. For visualization by TEM, 5 μl sample aliquots were absorbed to carbon-coated collodion film supported on 200-mesh copper grids, for 5 minutes, and negatively stained with 1% uranyl acetate. Grids were exhaustively examined with a JEOL JEM-1400 transmission electron microscope equipped with an Orious Sc1000 digital camera.

Cell culture and caspase-3 assay

SH-SY5Y cells (human neuroblastoma cell line; European Collection of Cell Cultures) were propagated in 25-cm^2 fasks and maintained at 37 ºC in a 95% humidified atmosphere and 5% CO_2. Cells were grown in Dulbecco's minimal essential medium supplemented with 10% fetal bovine serum (Gibco BRL). Activation of caspase-3 was measured using the CaspACE fuorimetric 96-well plate assay system (Sigma), following the manufacturer's instructions. Briefy, 10 μM A¡3(1-42) (Genscript) pre-incubated for 48 h at 4 ºC with shaking, in F12 media (Gibco BRL) with or without 2 μM TTR (alone or previously incubated with IDIF (20 μM) for 1 h at 37 ºC), were added to 80% confuent cells, cultured in 6-well plates, in Dulbecco's minimal essential medium with 1% fetal bovine serum, and further incubated for 24 h, at 37 ºC. Subsequently, each well was trypsinized and the cell pellet was lysed in 100 μl of hypotonic lysis buffer (Sigma). Forty μL of each cell lysate were used in duplicates for determination of caspase-3 activation. The remaining cell lysate was used to measure total cellular protein concentration with the Bio-Rad protein assay kit (Bio-Rad), using BSA as standard. Values shown are the mean of duplicates and the experiment was performed twice. Comparison between groups was made using the Student's t-test. A P value of less than 0.05 was considered statistically significant.

Acknowledgments

I. Cardoso worked under the Investigator FCT Program which is financed by national funds through FCT and co-financed by ESF through HPOP, type 4.2 – Promotion of Scientific Employment and currently works under the Program CEEC_Institucional_2017. G. Arsequell from IQAC-CSIC acknowledges a grant from Fundació Marató de TV3, Spain (Project ref. 20140330-31-32-33-34) and also acknowledges financial support from the Spanish Ministry of Economy (CTQ2016-76840-R). E.Y. Cotrina acknowledges a one year contract from Ford-Fundación Apadrina la Ciencia. The group at CIC bioGUNE acknowledges the European Research Council for financial support (ERC-2017-AdG, project number 788143-RECGLYC-ANMR), Instituto de Salud Carlos III of Spain, ISCIII (grant PRB3 IPT17/0019 to A. G.), Agencia Estatal Investigación of Spain, AEI (grants CTQ2015-64597-C2-1-P and RTI2018-094751-B-C21) and the Severo Ochoa Excellence Accreditation (SEV-2016-0644). Jordi Llop from CIC

biomaGUNE acknowledges the Spanish Ministry of Economy and Competitiveness for financial support through grant CTQ2017-87637-R. G. Arsequell from IQAC-CSIC acknowledges Dr. Maria José Bleda (CID-CSIC, Spain) for full support on statistical analysis, acknowledges Prof. Antoni Planas (IQS-URL) for full technical support and supervision on the TTR production; and acknowledges Dr. David Amabilino for language editing and revision of this manuscript.

Acknowledgments

Author contributions

E.Y.C., I. C., R. P. and G. A. conceived and designed the experiments; E.Y.C., R. P. and G. A. performed the experiments and data analysis; E.Y.C., J.L., A.G., J. J.-B., I. C., J. Q., R. P. and G. A. wrote and revised the manuscript.

Additional information

Supplementary information accompanies this paper at https://doi.org/...

Hard lessons from AD drug discovery; comparison to other assays; chemical compounds; wt rhTTR production and purification and MALDI-ToF MS; Amyloid peptides: synthesis of Aφ3(12-28) peptide, purification and characterization; preparation of Aφ3(1-42); Design of experiments; Method development and optimization; Turbidity assays of the binary and ternary assay complex formation up to 18h; ThT fluorescence assays of the binary and ternary assay complex with Aφ3(1-42); Morphological studies: TEM studies; ITC studies of the binary interaction (TTR+DCPA) and the ternary interaction [(TTR+DCPA)+ Aφ3(12-28)] and ITC studies of the binary interaction (TTR+DFPA) and the ternary interaction [(TTR+DFPA)+ Aφ3(12-28)].

Competing interests

The authors declare no competing interests.

Abbreviations

AD, Alzheimer's disease; A¡3, amyloid beta; BSA, Bovine Serum Albumin; DCPA, *N*-(3,5-dichlorophenyl)anthranilic; DFPA, *N*-(3,5-difluorophenyl)anthranilic; DIF, diflunisal; DMSO, dimethyl sulfoxide; DoE, Design of Experiments; HEPES, *N*-(2-hydroxyethyl) piperazine-N'-(2-ethanesulfonic acid); IDIF, iododiflunisal; HTS, High-Throughput Screening; IPTG, Isopropyl ¡3-D-1-thiogalactopyranoside; ITC, Isothermal Titration Calorimetry; MALDI-ToF MS, Matrix-assisted Laser Desorption/Ionization Time-of-Flight Mass Spectrometry; MW- SPPS, Microwave Solid-Phase Peptide Synthesis; NSAID, Non-Steroidal Anti-Inflammatory Drug; RA, reduction of aggregates; RP-HPLC, Reversed Phase High-Performance Liquid Chromatography; SDS-PAGE, Sodium Dodecyl Sulfate Polyacrylamide Gel Electrophoresis; SMCs, small-molecule chaperones; SPPS; Solid-Phase Peptide Synthesis; STD-NMR, Saturation Transfer Difference Nuclear Magnetic Resonance; TEM, Transmission Electron Microscopy TFA, Trifluoroacetic acid; TIS; *Tris*-isopropylsilane; Tris, Tris(hydroxymethyl)-aminomethane; UPLC-ToF MS, ultra-high performance liquid chromatography Time-of-Flight Mass Spectrometry; and wtTTR, wild-type transthyretin.

References

1. Blake, C. C.; Geisow, M. J.; Oatley, S. J.; Rerat, B.; Rerat, C. Structure of prealbumin: secondary, tertiary and quaternary interactions determined by Fourier refinement at 1.8 A. *J. Mol. Biol.* **1978**, *121*, 339-356.
2. Saraiva, M. J. Transthyretin amyloidosis: a tale of weak interactions, *FEBS Lett.* **2001***, 498*, 201-203.
3. Plante-Bordeneuve, V. Transthyretin familial amyloid polyneuropathy: an update. *J. Neurol.* **2018**, *265*, 976-983.
4. Pate, K. M.; Murphy, R. M. Cerebrospinal Fluid Proteins as Regulators of Beta-amyloid Aggregation and Toxicity. */sr. J. Chem.* **2017**, *57*, 602-612.
5. Davidsson, P.; Westman-Brinkmalm, A.; Nilsson, C. L.; Lindbjer, M.; Paulson, L.; Andreasen, N.; Sjógren, M.; Blennow, K. Proteome analysis of cerebrospinal fluid proteins in Alzheimer patients. *Neuroreport* **2002**, *13*, 611-615.
6. Serot, J. M.; Christmann, D.; Dubost, T.; Couturier, M. Cerebrospinal Fluid Transthyretin: Aging and Late Onset Alzheimer's Disease. *J. Neurol. Neurosurg. Psychiatry* **1997**, *63*, 506-550.
7. Ribeiro, C. A.; Santana, I.; Oliveira, C.; Baldeiras, I.; Moreira, J.; Saraiva, M. J.; Cardoso, I. Transthyretin decrease in plasma of MCI and AD patients: investigation of mechanisms for disease modulation. *Curr. Alzheimer Res.* **2012***, 9*, 881-889.
8. Han, S. H.; Jung, E. S.; Sohn, J. H.; Hong, H. J.; Hong, H. S.; Kim, J. W.; Na,D. L.; Kim, M.; Kim, H.; Ha, H. J.; Kim, Y. H.; Huh, N.; Jung, M. W.; Mook-Jung, I. Human Serum Transthyretin Levels Correlate Inversely with Alzheimer's Disease. *J. Alzheimers Dis.* **2011**, *25*, 77-84.
9. Nilsson, L.; Pamrén, A.; Islam, T.; Brannström, K.; Golchin, S. A.; Pettersson, N.; Iakovleva, I.; Sandblad, L.; Gharibyan, A. L.; Olofsson, A. ransthyretin Interferes with A¡3 Amyloid Formation by Redirecting Oligomeric Nuclei into Non-Amyloid Aggregates. *J. Mol. Biol.* **2018,** *430*, 2722-2733.
10. Ghadami, S. A.; Chia, S.; Ruggeri, F. S.; Meisl, G.; Bemporad, F.; Habchi, J.; Cascella, R.; Dobson, C. M.; Vendruscolo, M.; Knowles, T. P. J.; Chiti F. Transthyretin inhibits primary and secondary nucleation of amyloid-¡3 peptide aggregation and reduces the toxicity of its oligomers. *Biomacromolecules* **2020***, 21*, 1112-1125.
11. Ribeiro, C. A.; Saraiva, M. J.; Cardoso, I. Stability of the Transthyretin Molecule as a Key Factor in the Interaction with A-Beta Peptide-Relevance in Alzheimer's Disease. *PloS ONE* **2012**, 7 (9):e45368.
12. Almeida, M. R.; Macedo, B.; Cardoso, I.; Alves, I.; Valencia, G.; Arsequell, G.; Planas, A.; Saraiva, M. J. Selective binding to transthyretin and tetramer stabilization in serum from patients with familial amyloidotic polyneuropathy by an iodinated diflunisal derivative. *Biochem. J.* **2004**, *381*, 351-356.
13. Mairal, T.; Nieto, J.; Pinto, M.; Almeida, M. R.; Gales, L.; Ballesteros, A.; Barluenga, J.; Pérez, J. J.; Vázquez, J. T.; Centeno, N. B.; Saraiva, M. J.; Damas, A. M.; Planas, A.; Arsequell, G.; Valencia, G. Iodine atoms: a new molecular feature for the design of potent transthyretin fibrillogenesis inhibitors. *PLoS One* **2009***, 4***,** e4124.
14. Gales, L.; Macedo-Ribeiro, S.; Arsequell, G.; Valencia, G.; Saraiva, M. J.; Damas, A. M. Human transthyretin in complex with iododiflunisal: structural features associated with a potent amyloid inhibitor. *Biochem. J.* **2005***, 388*, 615-662.
15. Rios, X.; Gómez-Vallejo, V.; Martín, A.; Cossío, U.; Morcillo, M.Á.; Alemi, M.; Cardoso, I.; Quintana, J.; Jiménez-Barbero, J.; Cotrina, E.Y.; Valencia, G.; Arsequell, G.; Llop, J. Radiochemical examination of transthyretin (TTR) brain penetration assisted by iododiflunisal, a TTR tetramer stabilizer and a new candidate drug for AD. *Sci. Rep.* **2019,** 9(1) 13672.
16. Ribeiro, C. A.; Oliveira, S. M.; Guido, L. F.; Magalhaes, A.; Valencia, G.; Arsequell, G.; Saraiva, M. J.; Cardoso, I. Transthyretin stabilization by iododiflunisal promotes amyloid-¡3 peptide clearance, decreases its deposition, and ameliorates cognitive deficits in an Alzheimer's disease mouse model. *J. Alzheimers Dis.* **2014**, *39*, 357-370.
17. Gimeno, A.; Santos, L. M.; Alemi, M.; Rivas, J.; Blasi, D.; Cotrina, .Y.; Llop, J.; Valencia, G.; Cardoso, I.; Quintana, J.; Arsequell, G.; Jiménez-Barbero, J. Insights on the Interaction between Transthyretin and A¡3 in Solution. A Saturation Transfer Difference (STD) NMR Analysis of the Role of Iododiflunisal. *J. Med. Chem.* **2017**, *60*, 5749-5758.
18. Fraser, P. E.; Lévesque, L.; McLachlan D. R. Alzheimer A¡3 amyloid forms an inhibitory neuronal substrate. *J. Neurochem.* **1994***, 62*, 1227-1230.

19. Flood, J. F.; Morley, J. E.; Roberts E. An amyloid ¡3-protein fragment, Aφ3 (12-28), equipotently impairs post-training memory processing when injected into different limbic system structures. *Brain Res.* **1994**, *663*, 271-276.
20. Hsu, F.; Park, G.; Guo, Z. Key Residues for the Formation of A¡342 Amyloid Fibrils. *ACS Omega* **2018**, *3*, 8401-8407.
21. Daly, S.; Kulesza, A.; Poussigue, F.; Simon, A. L.; Choi C. M.; Knight, G.; Chirot, F.; MacAleese, L.; Antoine, R.; Dugourd, P. Conformational changes in amyloid-beta (12-28) alloforms studied using action-FRET, IMS and molecular dynamics simulations. *Chem. Sci.* **2015**, *6*, 5040-5047. Correction in: *Chem Sci.* **2016**, *7*, 1609-1610.
22. Jarvet, J.; Damberg, P.; Bodell, K.; Eriksson, L. E. G.; Graslund, A. Reversible Random Coil to ¡3-Sheet Transition and the Early Stage of Aggregation of the A¡3(12-28) Fragment from the Alzheimer Peptide. *J. Am. Chem. Soc.* **2000**, *122*, 4261-4268.
23. Jarvet, J.; Damberg, P.; Danielsson, J.; Johansson, I.; Eriksson, L. E.; Graslund, A. A left-handed 3(1) helical conformation in the Alzheimer Abeta(12-28) peptide. *FEBS Lett.* **2003**, *555*, 371-374.
24. Enache, T. A.; Chiorcea-Paquim, A. M.; Oliveira-Brett, A. M. Amyloid Beta Peptide VHHQ, KLVFF, and IIGLMVGGVV Domains Involved in Fibrilization: AFM and Electrochemical Characterization. *Anal. Chem.* **2018**, *90*, 2285-2292.
25. Liu, R.; McAllister, C.; Lyubchenko, Y.; Sierks, M. R. Residues 17-20 and 30-35 of beta-amyloid play critical roles in aggregation. *J. Neurosci. Res.* **2004**, *75*, 162-171.
26. Wood, S. J.; Wetzel, R.; Martin, J. D.; Hurle, M. R. Prolines and Amyloidogenicity in Fragments of the Alzheimer's Peptide beta/A4. *Biochemistry* **1995**, *34*, 724-730.
27. Fraser, P. E.; Nguyen, J. T.; Surewicz, W. K.; Kirschner, D. A. pH-dependent structural transitions of Alzheimer amyloid peptides. *Biophys. J.* **1991**, *60*, 1190-1201.
28. Mandal, P.; Eremina, N.; Barth, A. Formation of Two Different Types of Oligomers in the Early Phase of pH-Induced Aggregation of the Alzheimer A¡3(12-28) Peptide. *J. Phys. Chem. B.* **2012**, *116*, 12389-12397.
29. Golabek, A. A.; Marques, M.; Lalowski, M.; Wisniewski, T. Amyloid ¡3 binding proteins *in vitro* and in normal human cerebrospinal fluid. *Neurosci. Lett.* **1995**, *191*, 79-82.
30. Sadowski, M.; Pankiewicz, J.; Scholtzova, H.; Ripellino, J. A.; Li, Y.; Schmidt, S. D.; Mathews, P. M.; Fryer, J. D.; Holtzman, D. M.; Sigurdsson, E. M.; Wisniewski, T. A. Synthetic peptide blocking the apolipoprotein E/beta-amyloid binding mitigates beta-amyloid toxicity and fibril formation in vitro and reduces beta-amyloid plaques in transgenic mice. *Am. J. Pathol.* **2004**, *165*, 937-948.
31. Milojevic, J.; Esposito, V.; Das, R.; Melacini, G. Understanding the molecular basis for the inhibition of the Alzheimer's Abeta-peptide oligomerization by human serum albumin using saturation transfer difference and off-resonance relaxation NMR spectroscopy. *J. Am. Chem. Soc.* **2007**, *129*, 4282-4290.
32. Cotrina, E.Y.; Gimeno, A.; Llop, J.; Jiménez-Barbero, J.; Quintana, J.; Valencia, G.; Cardoso, I.; Prohens, R.; Arsequell, G. Calorimetric studies of binary and ternary molecular interactions between transthyretin, A¡3 peptides and small-molecule chaperones towards an alternative strategy for Alzheimer's Disease drug discovery. *J. Med. Chem.* **2020**, *63*, 3205-3214.
33. Dolado, I.; Nieto, J.; Saraiva, M. J. M.; Arsequell, G.; Valencia, G.; Planas A A Kinetic assay for high-throughput screening of in vitro transthyretin amyloid fibrillogenesis inhibitors. *J. Comb. Chem.* **2005**, *7*, 246-252.
34. Kuehl, R. O. *Design of experiments: statistical principles of research design and analysis*. 2nd ed.; Duxbury/Thomson Learning Pacific Grove: CA, **2000**.
35. Box, G. E. P.; Stuart Hunter, J.; Hunter, W.G. *Statistics for Experimenters: Design, /nnovation, and Discovery*. 2nd ed.; Wiley-Interscience: New Jersey, **2005**.
36. Ji, L.; Zhao, X.; Hua, Z. Potential therapeutic implications of gelsolin in Alzheimer's disease. *J. Alzheimers Dis.* **2015**, *44*, 13-25.
37. Nelson, A. R.; Sagare, A. P.; Zlokovic, B. V. Role of clusterin in the brain vascular clearance of amyloid-¡3. *Proc. Natl. Acad. Sci. U. S. A.* **2017**, *114*, 8681-8682.
38. Beeg, M.; M.; Stravalaci, M.; Romeo, M.; Carrá, A. D.; Cagnotto, A.; Rossi, A.; Diomede, L.; Salmona, M.; Gobbi, M. Clusterin Binds to A¡31-42 Oligomers with High Affinity and Interferes with Peptide Aggregation by Inhibiting Primary and Secondary Nucleation. *J. Biol. Chem.* **2016**, *291*, 6958-6966.

39. Liu, S.; S.; Park, S.; Allington, G.; Prelli, F.; Sun, Y.; Martá-Ariza, M.; Scholtzova, H.; Biswas, G.; Brown, B.; Verghese, P. B.; Mehta, P. D.; Kwon, Y. U.; Wisniewski, T. Targeting Apolipoprotein E/Amyloid ¡3 Binding by Peptoid CP0_A¡317-21 P Ameliorates Alzheimer's Disease Related Pathology and Cognitive Decline. *Sci. Rep*. **2017**, *7*:8009.
40. Boada, M.; López, O.; Núñez, L.; Szczepiorkowski, Z. M.; Torres, M.; Grifols, C.; Páez, A. Plasma exchange for Alzheimer's disease Management by Albumin Replacement (AMBAR) trial: Study design and progress. *Alzheimers Dement.* (N Y). **2019**, *5*, 61-69.
41. Algamal, M.; Ahmed, R.; Jafari, N.; Ahsan, B.; Ortega, J.; Melacini, G. Atomic-resolution map of the interactions between an amyloid inhibitor protein and amyloid ¡3 (A¡3) peptides in the monomer and protofibril states. *J. Biol.Chem.* **2017**, *292*, 17158-17168.
42. Wurth, C.; Guimard, N. K.; Hecht, M. H. Mutations that reduce aggregation of the Alzheimer's Abeta42 peptide: an unbiased search for the sequence determinants of Abeta amyloidogenesis. *J. Mol. Biol.* **2017**, 319, 1279-1290.
43. Roostaee, A.; Côté, S.; Roucou X. Aggregation and amyloid fibril formation induced by chemical dimerization of recombinant prion protein in physiological-like conditions. *J. Biol. Chem.* **2009**, *284*, 30907-30916.
44. López, L.C.; Dos-Reis, S.; Espargaró, A.; Carrodeguas, J. A.; Maddelein, M. L.; Ventura, S.; Sancho, J. Discovery of novel inhibitors of amyloid ¡3-peptide 1-42 aggregation. *J. Med. Chem.* **2012**, *55*, 9521-9530.
45. *JMP* ®, Version *12.1.0*. *SAS* Institute Inc., Cary, NC, USA.
46. Wilcoxon, F. Individual comparisons by ranking methods. *Biometrics* **1945***, 1*, 80-83.
47. Zhang, J. H.; Chung, T. D.; Oldenburg, K. R. A. Simple Statistical Parameter for Use in Evaluation and Validation of High Throughput Screening Assays. *J. Biomol. Screen.* **1999**, *4*, 67-73.
48. LeVine H 3rd. Thioflavine T interaction with synthetic Alzheimer's disease beta-amyloid peptides: detection of amyloid aggregation in solution. *Protein Sci*. **1993**, *2*, 404-410.
49. Costa, R; Goncalves, A.; Saraiva, M. J.; Cardoso, I. Transthyretin binding to A-Beta peptide--impact on A-Beta fibrillogenesis and toxicity. *FEBS Lett.* **2008**, *582*, 936-942.